

# UCLA

## UCLA Previously Published Works

### Title

Crystal structure of the  $\alpha 6\beta 6$  holoenzyme of propionyl-coenzyme A carboxylase

### Permalink

<https://escholarship.org/uc/item/7x89r678>

### Journal

Nature, 466(7309)

### ISSN

0028-0836

### Authors

Huang, Christine S  
Sadre-Bazzaz, Kianoush  
Shen, Yang  
[et al.](#)

### Publication Date

2010-08-01

### DOI

10.1038/nature09302

Peer reviewed



Published in final edited form as:

Nature. 2010 August 19; 466(7309): 1001–1005. doi:10.1038/nature09302.

## Crystal structure of the $\alpha_6\beta_6$ holoenzyme of propionyl-coenzyme A carboxylase

Christine S. Huang<sup>1,\*</sup>, Kianoush Sadre-Bazzaz<sup>1,\*</sup>, Yang Shen<sup>1,4</sup>, Binbin Deng<sup>2</sup>, Z. Hong Zhou<sup>2,3</sup>, and Liang Tong<sup>1</sup>

<sup>1</sup> Department of Biological Sciences, Columbia University, New York, NY 10027, USA

<sup>2</sup> Department of Pathology and Laboratory Medicine, University of Texas Medical School at Houston, Houston, TX 77030, USA

<sup>3</sup> Department of Microbiology, Immunology and Molecular Genetics, University of California, Los Angeles, Los Angeles, CA 90095, USA

### Abstract

Propionyl-coenzyme A carboxylase (PCC), a mitochondrial biotin-dependent enzyme, is essential for the catabolism of the amino acids Thr, Val, Ile and Met, cholesterol, and fatty acids with an odd number of carbon atoms. Deficiencies of PCC activity in humans are linked to the disease propionic acidemia (PA), an autosomal recessive disorder that can be fatal in infants<sup>1–4</sup>. The holoenzyme of PCC is an  $\alpha_6\beta_6$  dodecamer, with a molecular weight of 750 kD. The  $\alpha$  subunit contains the biotin carboxylase (BC) and biotin carboxyl carrier protein (BCCP) domains, while the  $\beta$  subunit supplies the carboxyltransferase (CT) activity. Here we report the crystal structure at 3.2 Å resolution of a bacterial PCC  $\alpha_6\beta_6$  holoenzyme as well as cryo-electron microscopy (cryo-EM) reconstruction at 15 Å resolution demonstrating a similar structure for human PCC. The structure defines the overall architecture of PCC and reveals unexpectedly that the  $\alpha$  subunits are arranged as monomers in the holoenzyme, decorating a central  $\beta_6$  hexamer. A hitherto unrecognized domain in the  $\alpha$  subunit, formed by residues between the BC and BCCP domains, is crucial for interactions with the  $\beta$  subunit. We have named it the BT domain. The structure reveals for the first time the relative positions of the BC and CT active sites in the holoenzyme. They are separated by approximately 55 Å, indicating that the entire BCCP domain must translocate during catalysis. The BCCP domain is located in the active site of the  $\beta$  subunit in the current structure, providing insight for its involvement in the CT reaction. The structural information establishes a molecular basis for understanding the large collection of disease-causing mutations in PCC, and also has important relevance for the holoenzymes of other biotin-dependent carboxylases,

Users may view, print, copy, download and text and data-mine the content in such documents, for the purposes of academic research, subject always to the full Conditions of use: [http://www.nature.com/authors/editorial\\_policies/license.html#terms](http://www.nature.com/authors/editorial_policies/license.html#terms)

Correspondence and requests for materials should be addressed to L.T. (ltong@columbia.edu).

\*These authors contributed equally to this work.

<sup>4</sup>Present address: Department of Antibody Technology, ImClone Systems, a wholly-owned subsidiary of Eli Lilly and Company, 180 Varick St., 6<sup>th</sup> Floor, New York, NY 10014, USA.

Supplementary Information is linked to the online version of the paper at [www.nature.com/nature](http://www.nature.com/nature).

**Author Information.** The atomic coordinates have been deposited at the Protein Data Bank (accession code 3N6R). Reprints and permissions information are available at [www.nature.com/reprints](http://www.nature.com/reprints). The authors declare no competing financial interests.

including 3-methylcrotonyl-CoA carboxylase (MCC)<sup>5-7</sup> and eukaryotic acetyl-CoA carboxylase (ACC)<sup>8,9</sup>.

### Keywords

fatty acid metabolism; amino acid metabolism; propionic acidemia; 3-methylcrotonylglycinuria; protein complex; biotin-dependent carboxylase; acetyl-CoA carboxylase; 3-methylcrotonyl-CoA carboxylase

PCCs catalyze the carboxylation of propionyl-CoA to produce *D*-methylmalonyl-CoA. These enzymes are found from bacteria to humans, with highly conserved amino acid sequences. For example, the  $\alpha$  and  $\beta$  subunits of human PCC (HsPCC) and *Ruegeria pomeroyi* PCC (RpPCC) share 54% and 65% sequence identity, respectively (Supplementary Figs. 1, 2). To simplify discussions, we have numbered residues in bacterial PCCs according to their equivalents in HsPCC. The BC and BCCP domains in the  $\alpha$  subunit are homologous to their equivalents in ACC and pyruvate carboxylase (PC), while the  $\beta$  subunit is homologous to the CT domain of ACC. The active site of BC is formed by residues from its A and C (sub-)domains, while the B (sub-)domain forms a lid that can assume open and closed conformations<sup>9-11</sup>. The active site of CT is located at the interface of its dimer, and each CT contains two (sub-)domains, N and C domains<sup>9,12</sup>. In contrast to the wealth of information about these domains, little is known about how they are assembled into the holoenzyme of PCC (or ACC).

After extensive efforts (Supplementary text), we determined the crystal structure of a PCC chimera, containing the  $\alpha$  subunit of RpPCC and the  $\beta$  subunit of *Roseobacter denitrificans* PCC (RdPCC) (Supplementary Table 1). The structure of the chimera is essentially the same as that of the native RpPCC dodecamer (Supplementary text) as well as that of the HsPCC holoenzyme (see below).

The structure of the  $\alpha_6\beta_6$  PCC holoenzyme contains a central  $\beta_6$  hexamer core, in the shape of a short cylinder with a small hole along its axis (Fig. 1a). This hexameric core can be considered as a trimer of  $\beta_2$  dimers, with each dimer being formed by one subunit from each layer of the structure (Fig. 1b). In contrast, the  $\alpha$  subunits are arranged as monomers on both ends of the  $\beta_6$  core, far from the center of the holoenzyme, with each  $\alpha$  subunit contacting primarily only one  $\beta$  subunit (see below). There are no significant conformational differences among the six copies of the  $\alpha$  and  $\beta$  subunits of the holoenzyme (Supplementary text).

We carried out cryo-EM studies on HsPCC and obtained a 3D reconstruction at 15 Å resolution by single particle analysis (Supplementary Figs. 3–6). The cryo-EM envelope is remarkably similar to the overall shape of the crystal structure (Fig. 1c). In fact, the atomic model can be readily fit into the cryo-EM map, giving a cross-correlation value of 0.80, and only the BCCP domain appears to be in a somewhat different position (Fig. 1d). These studies demonstrate that the structure of HsPCC is highly similar to that of the bacterial enzyme.

An unexpected discovery from the crystal structure of the holoenzyme is that there is little direct contact between the BC domain in the  $\alpha$  subunit and the  $\beta$  subunit (Fig. 2a). Instead, interactions with the  $\beta$  subunit are primarily mediated by a hitherto unrecognized domain in the  $\alpha$  subunit, formed by residues 514–653 in the connection between the BC and BCCP domains (Supplementary Fig. 1). We have named it the BT domain, as it mediates BC-CT interactions. The BT domain has well-defined electron density (Supplementary Fig. 7), suggesting that it is highly ordered in the holoenzyme. A total of 1,950 Å<sup>2</sup> of the surface area of each  $\alpha$  subunit is buried at the interface with the  $\beta$  subunits. Only 200 Å<sup>2</sup> are contributed by the BC domain (Fig. 2a). In contrast, the BT domain contributes 1,300 Å<sup>2</sup> to the buried surface area with one  $\beta$  subunit, and an additional 100 Å<sup>2</sup> with an adjacent  $\beta$  subunit (Fig. 2a). Finally, the BCCP domain contributes 350 Å<sup>2</sup> to the interface (see below).

The BT domain contains a long helix ( $\alpha$ V, Supplementary Fig. 1) at the N-terminus, followed by an eight-stranded up-down  $\beta$ -barrel ( $\beta$ 22- $\beta$ 29) that surrounds the N-terminal two-thirds of the helix (Fig. 2a, Supplementary Fig. 8). The C-terminal one-third of the helix and the long loop connecting to the first  $\beta$ -strand protrude from the  $\beta$ -barrel, and form a 'hook' that provides a major contact with the  $\beta$  subunit (Fig. 2b, Supplementary Fig. 8). A second area of close contact with the  $\beta$  subunit is mediated by a small helix ( $\alpha$ W) at the end of the BT domain (Fig. 2c, Supplementary Fig. 8), which projects away from the  $\beta$ -barrel (Fig. 2a). The BT domain does not have any close structural homologs in the Protein Data Bank, based on an analysis with the program DaliLite<sup>13</sup>. Remarkably, however, the domain does share some structural similarity with the PT domain of PC, which helps mediate the tetramerization of that enzyme (Supplementary text, Supplementary Fig. 9)<sup>14</sup>.

A large number of residues are located in the interface between the  $\alpha$  and  $\beta$  subunits (Supplementary Figs. 1 and 2), forming ion-pair, hydrogen-bonding and hydrophobic interactions (Supplementary text). Residues making important contributions to the interface are generally conserved or show conservative variations among the PCC enzymes (Supplementary Figs. 1 and 2), consistent with our observations that HsPCC has a similar structure. Our mutagenesis data confirm the extensive nature of the  $\alpha$ - $\beta$  subunit interface and suggest that the holoenzyme can withstand substantial disruptions in it (Supplementary text, Supplementary Table 2).

Another unexpected discovery from the structure is that the BC domains are arranged as monomers in the PCC holoenzyme (Fig. 1a). Studies of the BC subunit of bacterial ACCs have shown a dimeric association<sup>9–11</sup>, which may be required for its activity<sup>15</sup>, although monomeric BC mutants are catalytically active<sup>16</sup>. A conserved dimeric association of the BC domain was also observed in PC<sup>14,17</sup>. However, the BC domains in PCC are monomeric and, in fact, there are no contacts among the  $\alpha$  subunits in the holoenzyme (Fig. 1a). Our structure defines the molecular basis for the lack of dimerization of the BC domain in PCC (Supplementary text). A monomeric arrangement of the BC domains also has significant relevance for the holoenzyme of eukaryotic ACCs (see below).

The active site of the BC domain is conserved with that of *E. coli* BC, and all the residues that interact with the substrates of this reaction have essentially the same conformation in both structures (Supplementary Fig. 10)<sup>18</sup>. Similarly, residues in the active site of CT,

located at the interface of a  $\beta$  subunit dimer (Fig. 3a), are also conserved. The structure of this dimer is homologous to those of the *S. coelicolor* and *M. tuberculosis* acyl-CoA carboxylase  $\beta$  subunits<sup>19,20</sup> and the 12S subunit of *P. shermanii* transcarboxylase (Supplementary Fig. 11)<sup>21</sup>, which also form similar hexamers. Weaker structural similarity is observed with the CT domain of yeast ACC<sup>12</sup>, the CT subunit of bacterial ACC<sup>22</sup>, and the CT subunit of a bacterial sodium pump<sup>23</sup>, although these CT enzymes only form dimers. A helical sub-domain at the C-terminus of the CT domain of ACC is incompatible with the  $\beta_6$  hexamer of PCC.

Our structure reveals for the first time the relative positions of the BC and CT active sites in the holoenzyme, providing unprecedented insight into PCC catalysis. The distance between the two active sites in PCC is about 55 Å (Fig. 3a), and consequently the entire BCCP domain must translocate during catalysis (Supplementary text, Supplementary Fig. 12). A similar situation has been observed in the structure of PC, where the BC and CT active sites are separated by 75 Å<sup>14,17</sup>. Our cryo-EM studies on HsPCC have provided direct experimental evidence that the BCCP domain can be located in different positions in the holoenzyme (Fig. 1d). Residues 654–660, the linker between the BT and BCCP domains, have weak electron density and are exposed to the solvent in the current structure (Fig. 1b), suggesting that they are flexible and can facilitate the translocation.

Further insight into PCC catalysis is obtained from the binding of the BCCP domain and its associated biotin, with well-defined electron density (Supplementary Fig. 13), in the CT active site (Fig. 3a). The interface between BCCP and the  $\beta$  subunit is small, with 350 Å<sup>2</sup> surface area burial. Only residues 693–697 around the biotinylation site (Lys694) interact with the  $\beta$  subunit, through hydrophobic interactions and one hydrogen bond (Fig. 3b, Supplementary Fig. 14). This weak interaction should also help the BCCP domain to leave the CT active site and translocate to the BC active site during catalysis.

The active site of CT is located in a deep canyon at the  $\beta$  subunit dimer interface (Fig. 3c). The  $\alpha_6$  helix from the C domain of one subunit and the  $\alpha_6$  helix from the N domain of the other subunit form the two walls of the canyon. Our structure shows that BCCP-biotin occupies one half of the canyon, interacting with the C domain of one subunit (Fig. 3d, Supplementary Fig. 14). Propionyl-CoA, the other substrate of this activity, is expected to occupy the other half of the canyon and interact with the N domain of the second  $\beta$  subunit (Fig. 3d)<sup>12,19,21</sup>, with the propionyl group located in the center of the canyon (Fig. 3c). Biotin is in a partially folded, unproductive conformation in the current structure (Fig. 3b), although a conformational change in the side chain of Lys694 and the valeryl group of biotin should readily bring the N1' atom into the proximity of propionyl-CoA for catalysis.

The structure of the holoenzyme establishes a foundation for understanding the molecular basis of the large number of disease-causing mutations in PCC (Fig. 4, Supplementary Table 3)<sup>1–4</sup>. Among these, only the R399Q mutation in the  $\alpha$  subunit directly disrupts a residue in the active site (Supplementary Fig. 15). This side chain stabilizes the biotin enolate during BC catalysis (Supplementary Fig. 10)<sup>18</sup>, and the mutation leads to a large loss in activity<sup>18,24</sup>. Another mutation, G668R in the BCCP domain (Fig. 4), abolishes biotinylation. Many of the other mutations are detrimental to catalysis by destabilizing the enzyme and/or

interfering with holoenzyme assembly<sup>1,25-27</sup>. A large number of them, especially those in the  $\beta$  subunit, are actually located near the active site (Supplementary Fig. 15), and they may indirectly affect substrate binding and/or catalysis as well. For example, the R165W and R165Q mutations may disturb the recognition of the adenine base of CoA (Supplementary Fig. 15). On the other hand, few of the missense mutations are located in the interface between the  $\alpha$  and  $\beta$  subunits of the holoenzyme (Fig. 4, Supplementary 16). The extensive nature of this interface makes it difficult to disrupt the holoenzyme by single-site mutations in this region (Supplementary text).

The structure of the PCC holoenzyme also has strong implications for the structure and function of other biotin-dependent carboxylases. There are five such enzymes in humans: PCC, MCC, ACC1, ACC2 and PC (Supplementary Fig. 17). MCC is a close homolog of PCC, with the same domain architecture and subunit organization. Therefore, the PCC structure is directly relevant for understanding the MCC enzyme and its disease-causing mutations<sup>5-7</sup>.

Most importantly, the identification of the BT domain in PCC led us to reexamine the sequences of eukaryotic, multi-domain ACCs. The segment containing the BC and BCCP domains in these enzymes is remarkably similar to the PCC  $\alpha$  subunit, with a linker of about 120 residues between the two domains (Supplementary Fig. 17). Secondary structure prediction shows that this linker contains a helix followed by seven or more  $\beta$ -strands, suggesting that it may form a structure similar to the BT domain in PCC. This putative BT domain of ACC is likely also crucial for mediating interactions between its BC and CT domains. In fact, we have observed that purified BC and CT domains of yeast ACC do not interact with each other (unpublished results). Since the CT domain dimer of ACC is similar to the  $\beta_2$  dimer of PCC, the  $\alpha_2\beta_2$  assembly of PCC might be a plausible model for the organization of the ACC dimer, the protomer that can also form higher oligomers. This model implies that the BC domain could be monomeric in the ACC holoenzyme, which is consistent with observations that isolated BC domains of eukaryotic ACCs are monomeric in solution<sup>28,29</sup>, in contrast to the dimers for bacterial BC subunits. Therefore, there might be a fundamental difference between the overall architecture of eukaryotic, multi-domain ACCs and that of bacterial, multi-subunit ACCs.

## Methods summary

### Crystallography

The  $\alpha$  and  $\beta$  subunits of PCC were co-expressed in *E. coli*, with a His-tag on the  $\beta$  subunit. The PCC holoenzyme was purified by nickel affinity and gel filtration chromatography. Crystals were obtained by the microbatch method under oil, and the structures were determined by the molecular replacement method.

### Cryo-electron microscopy

Frozen hydrated human PCC particles at 70  $\mu\text{g/ml}$  concentration were imaged at 50,000 $\times$  magnification in a 100 kV cryo-electron microscope. A featureless Gaussian oval was used to obtain a low resolution (40  $\text{\AA}$ ) model from negative stain electron microscope images. A

15 Å resolution 3D reconstruction was obtained from ~10,000 cryo-EM particle images, using the structure from the negative stain images as the initial model.

### Mutagenesis and kinetic studies

Site-specific and deletion mutants were designed based on the structural information, and their effects on the formation of the holoenzyme was assessed by nickel affinity chromatography. The catalytic activity of PCC was determined by a coupled enzyme assay, monitoring the hydrolysis of ATP.

Full Methods and any associated references are available in the online version of the paper at [www.nature.com/nature](http://www.nature.com/nature).

### Supplementary Material

Refer to Web version on PubMed Central for supplementary material.

### Acknowledgments

We thank Neil Whalen and Howard Robinson for access to the X29A beamline at the NSLS; John Schwanof and Randy Abramowitz for access to the X4A beamline; Manan Sampat for help during the initial stages of the project; and W.W. Cleland for helpful discussions. This research was supported in part by NIH grants DK067238 (to LT), GM071940 and AI069015 (to ZHZ). CSH was also supported by an NIH training program in molecular biophysics (GM08281).

### References

1. Desviat LR, et al. Propionic acidemia: mutation update and functional and structural effects of the variant alleles. *Mol Gen Metab*. 2004; 83:28–37.
2. Rodriguez-Pombo P, et al. Towards a model to explain the intragenic complementation in the heteromultimeric protein propionyl-CoA carboxylase. *Biochim Biophys Acta*. 2005; 1740:489–498. [PubMed: 15949719]
3. Deodato F, Boenzi S, Santorelli FM, Dionisi-Vici C. Methylmalonic and propionic aciduria. *Am J Med Genet C Semin Med Genet*. 2006; 142:104–112. [PubMed: 16602092]
4. Desviat LR, et al. New splicing mutations in propionic acidemia. *J Hum Genet*. 2006; 51:992–997. [PubMed: 17051315]
5. Desviat LR, et al. Functional analysis of MCCA and MCCB mutations causing methylcrotonylglycinuria. *Mol Gen Metab*. 2003; 80:315–320.
6. Stadler SC, et al. Newborn screening for 3-methylcrotonyl-CoA carboxylase deficiency: population heterogeneity of MCCA and MCCB mutations and impact on risk assessment. *Human Mutation*. 2006; 27:748–759. [PubMed: 16835865]
7. Stucki M, Suormala T, Fowler B, Valle D, Baumgartner MR. Cryptic exon activation by disruption of exon splice enhancer. Novel mechanism causing 3-methylcrotonyl-CoA carboxylase deficiency. *J Biol Chem*. 2009; 284:28953–28957. [PubMed: 19706617]
8. Wakil SJ, Stoops JK, Joshi VC. Fatty acid synthesis and its regulation. *Ann Rev Biochem*. 1983; 52:537–579. [PubMed: 6137188]
9. Tong L. Acetyl-coenzyme A carboxylase: crucial metabolic enzyme and attractive target for drug discovery. *Cell Mol Life Sci*. 2005; 62:1784–1803. [PubMed: 15968460]
10. Waldrop GL, Rayment I, Holden HM. Three-dimensional structure of the biotin carboxylase subunit of acetyl-CoA carboxylase. *Biochem*. 1994; 33:10249–10256. [PubMed: 7915138]
11. Cronan JE Jr, Waldrop GL. Multi-subunit acetyl-CoA carboxylases. *Prog Lipid Res*. 2002; 41:407–435. [PubMed: 12121720]

12. Zhang H, Yang Z, Shen Y, Tong L. Crystal structure of the carboxyltransferase domain of acetyl-coenzyme A carboxylase. *Science*. 2003; 299:2064–2067. [PubMed: 12663926]
13. Holm L, Kaariainen S, Rosenstrom P, Schenkel A. Searching protein structure databases with DaliLite v.3. *Bioinformatics*. 2008; 24:2780–2781. [PubMed: 18818215]
14. Xiang S, Tong L. Crystal structures of human and *Staphylococcus aureus* pyruvate carboxylase and molecular insights into the carboxyltransfer reaction. *Nat Struct Mol Biol*. 2008; 15:295–302. [PubMed: 18297087]
15. Janiyani K, Bordelon T, Waldrop GL, Cronan JE Jr. Function of *Escherichia coli* biotin carboxylase requires catalytic activity of both subunits of the homodimer. *J Biol Chem*. 2001; 276:29864–29870. [PubMed: 11390406]
16. Shen Y, Chou CY, Chang GG, Tong L. Is dimerization required for the catalytic activity of bacterial biotin carboxylase? *Mol Cell*. 2006; 22:807–818. [PubMed: 16793549]
17. St Maurice M, et al. Domain architecture of pyruvate carboxylase, a biotin-dependent multifunctional enzyme. *Science*. 2007; 317:1076–1079. [PubMed: 17717183]
18. Chou C-Y, Yu LPC, Tong L. Crystal structure of biotin carboxylase in complex with substrates and implications for its catalytic mechanism. *J Biol Chem*. 2009
19. Diacovich L, et al. Crystal structure of the b-subunit of acyl-CoA carboxylase: structure-based engineering of substrate specificity. *Biochem*. 2004; 43:14027–14036. [PubMed: 15518551]
20. Lin TW, et al. Structure-based inhibitor design of AccD5, an essential acyl-CoA carboxylase carboxyltransferase domain of *Mycobacterium tuberculosis*. *Proc Natl Acad Sci USA*. 2006; 103:3072–3077. [PubMed: 16492739]
21. Hall PR, et al. Transcarboxylase 12S crystal structure: hexamer assembly and substrate binding to a multienzyme core. *EMBO J*. 2003; 22:2334–2347. [PubMed: 12743028]
22. Bilder P, et al. The structure of the carboxyltransferase component of acetyl-CoA carboxylase reveals a zinc-binding motif unique to the bacterial enzyme. *Biochem*. 2006; 45:1712–1722. [PubMed: 16460018]
23. Wendt KS, Schall I, Huber R, Buckel W, Jacob U. Crystal structure of the carboxyltransferase subunit of the bacterial sodium ion pump glutacetyl-coenzyme A decarboxylase. *EMBO J*. 2003; 22:3493–3502. [PubMed: 12853465]
24. Sloane V, Waldrop GL. Kinetic characterization of mutations found in propionic acidemia and methylcrotonylglycinuria. *J Biol Chem*. 2004; 279:15772–15778. [PubMed: 14960587]
25. Jiang H, Rao KS, Yee VC, Kraus JP. Characterization of four variant forms of human propionyl-CoA carboxylase expressed in *Escherichia coli*. *J Biol Chem*. 2005; 280:27719–27727. [PubMed: 15890657]
26. Muro S, et al. Effect of PCCB gene mutations on the heteromeric and homomeric assembly of propionyl-CoA carboxylase. *Mol Gen Metab*. 2001; 74:476–483.
27. Perez-Cerda C, et al. Functional analysis of PCCB mutations causing propionic acidemia based on expression studies in deficient human skin fibroblasts. *Biochim Biophys Acta*. 2003; 1638:43–49. [PubMed: 12757933]
28. Shen Y, Volrath SL, Weatherly SC, Elich TD, Tong L. A mechanism for the potent inhibition of eukaryotic acetyl-coenzyme A carboxylase by soraphen A, a macrocyclic polyketide natural product. *Mol Cell*. 2004; 16:881–891. [PubMed: 15610732]
29. Weatherly SC, Volrath SL, Elich TD. Expression and characterization of recombinant fungal acetyl-CoA carboxylase and isolation of a soraphen-binding domain. *Biochem J*. 2004; 380:105–110. [PubMed: 14766011]
30. Pettersen EF, et al. UCSF Chimera—a visualization system for exploratory research and analysis. *J Comput Chem*. 2004; 25:1605–1612. [PubMed: 15264254]



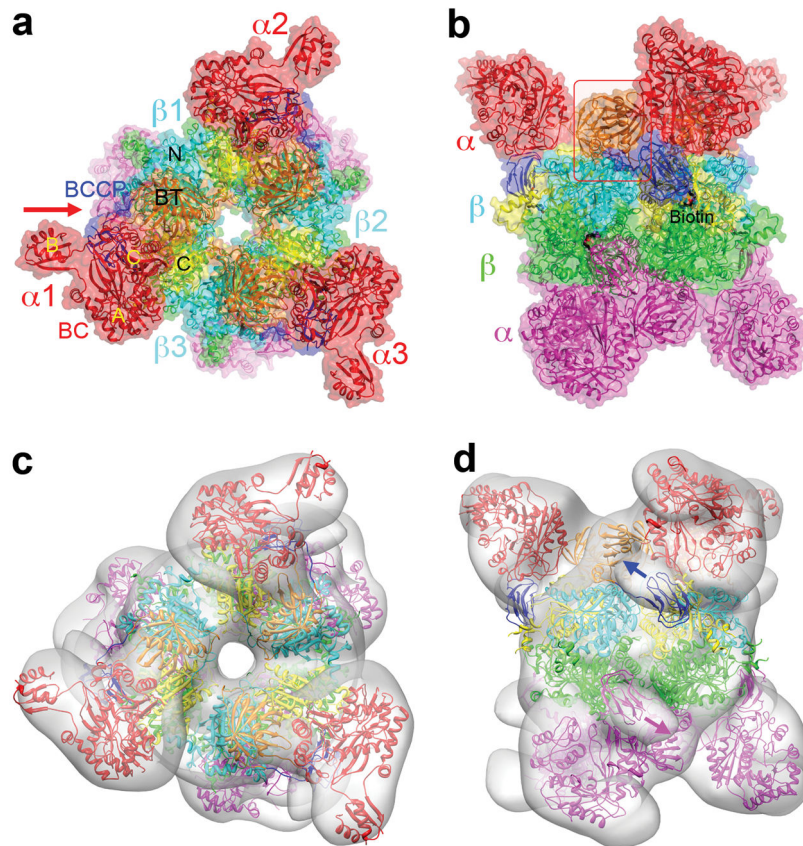


**Figure 1. Structure of the PCC holoenzyme**

(a). Schematic drawing of the structure of the RpPCC $\alpha$ -RdPCC $\beta$  chimera, viewed down the three-fold symmetry axis. Domains in the  $\alpha$  and  $\beta$  subunits in the top half of the structure are given different colors, and those in the first  $\alpha$  and  $\beta$  subunits are labeled. The  $\alpha$  and  $\beta$  subunits in the bottom half are colored in magenta and green, respectively. The red arrow indicates the viewing direction of panel b. (b). Structure of the RpPCC $\alpha$ -RdPCC $\beta$  chimera, viewed down the two-fold symmetry axis. The red rectangle indicates the region shown in detail in Fig. 2a. (c). Cryo-EM reconstruction of HsPCC at 15 Å resolution, viewed in the same orientation as panel a. The atomic model of the chimera was fit into the cryo-EM envelope. (d). The cryo-EM reconstruction viewed in the same orientation as panel b. The arrows indicate a change in the BCCP position that is needed to fit the cryo-EM map. All the structure figures were produced with PyMOL ([www.pymol.org](http://www.pymol.org)), and the cryo-EM figures were produced with Chimera<sup>30</sup>.

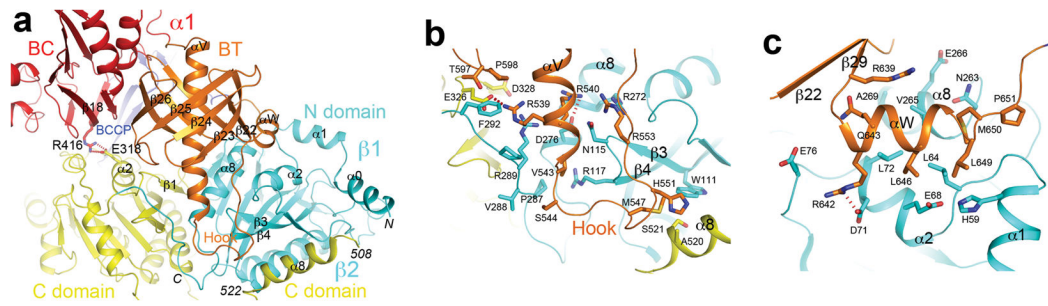


**Figure 2. Interactions between the  $\alpha$  and  $\beta$  subunits in the PCC holoenzyme**

(a). Schematic drawing of the interface between the  $\alpha$  and  $\beta$  subunits in the RpPCC $\alpha$ -RdPCC $\beta$  chimera. (b). Detailed interactions between the hook in the BT domain of the  $\alpha$  subunit and the  $\beta$  subunits. The C-terminal helix ( $\alpha 8$ ) of an adjacent  $\beta$  subunit (labeled  $\beta 2$ ) is also shown. (c). Detailed interactions between helix  $\alpha W$  in the BT domain and the  $\beta$  subunit. The view is related to that of panel a through a 90° rotation around the vertical axis. See Supplementary Fig. 8 for stereo versions of panels b and c.

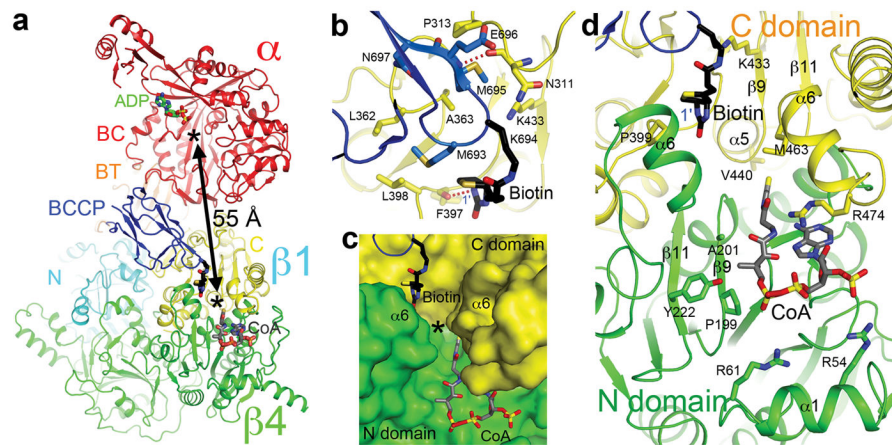


**Figure 3. The active sites of the PCC holoenzyme**

(a). Schematic drawing of the relative positioning of the BC and CT active sites in the holoenzyme. One  $\alpha$  subunit and a  $\beta_2$  dimer ( $\beta_1$  from one layer and  $\beta_4$  from the other layer) are shown, and the viewing direction is the same as Fig. 1b. The two active sites are indicated with the stars, separated by 55 Å distance. The bound positions of ADP in complex with *E. coli* BC<sup>18</sup> and that of CoA in complex with the 12S subunit of transcarboxylase<sup>21</sup> are also shown. (b). Detailed interactions between BCCP-biotin and the C domain of a  $\beta$  subunit. Hydrogen-bonding interactions are indicated with the dashed lines in red. The N1' atom of biotin is labeled as 1', hydrogen-bonded to the main-chain carbonyl of Phe397. (c). Molecular surface of the CT active site, showing a deep canyon where both substrates are bound. (d). Schematic drawing of the CT active site. See Supplementary Fig. 14 for stereo versions of panels b and d.

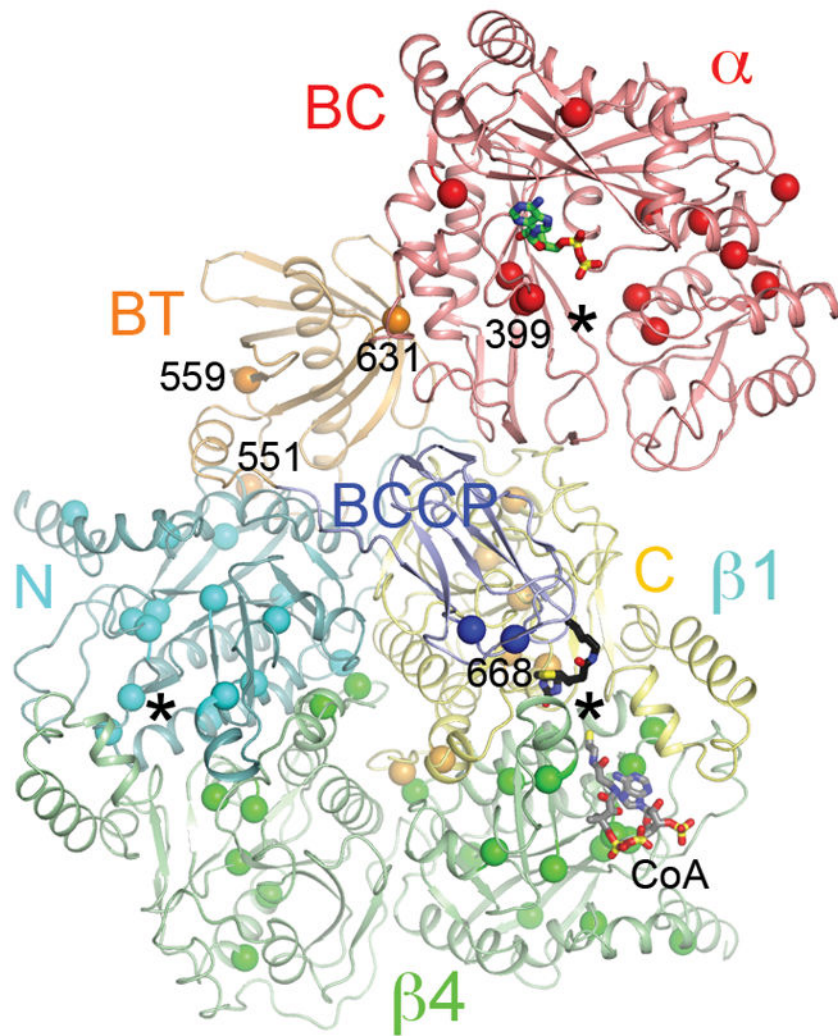


**Figure 4. Locations of disease-causing mutations in the PCC holoenzyme**

Schematic drawing of the structure of one  $\alpha$  subunit and one  $\beta_2$  subunit dimer of PCC, in the same view as Fig. 3a. The locations of the missense mutations associated with PA are indicated with the spheres, colored by the domains. The BC and CT active sites are indicated with the stars.